

Received 20 February 2018; accepted 22 May 2018. Date of publication 29 May 2018; date of current version 15 June 2018.
The review of this paper was arranged by Editor K. Shenai.

Digital Object Identifier 10.1109/JEDS.2018.2841374

Contactless Method to Measure 2DEG Charge Density and Band Structure in HEMT Structures

YURY TURKULETS AND ILAN SHALISH^{ID}

Department of Electrical Engineering, Ben-Gurion University of the Negev, Beer Sheva 8410501, Israel

CORRESPONDING AUTHOR: I. SHALISH (e-mail: shalish@bgu.ac.il)

This work was supported by the Israel Ministry of Defense (MAFAT).

ABSTRACT We present a contactless method capable of characterizing a high electron mobility transistor (HEMT) heterostructure at the wafer stage, right after its growth, before any production process has been attempted, to provide the equilibrium band structure and the density of charge of the 2-D electron gas in the quantum well (QW). The method can thus evaluate critical transistor parameters and help to screen out low performance wafers before the actual fabrication. To this end, we use a simple optical spectroscopy at room temperature that measures the surface photovoltage band-edge responses in the heterostructure and uses a model that takes into account the effect of the built-in electric fields on optical absorption in the layers and heterojunctions to evaluate bandgaps, band offsets, and built-in fields. The QW charge is then calculated from the built-in fields. The main advantage of the method is in its capability to provide information on all the different layers in the typical heterostructure simultaneously in a single measurement. The method is not limited to the HEMT structure but may be used on any other heterostructure. It opens the door for a new type of characterization methods suitable for the post-silicon multi-layer multi-semiconductor heterostructure device era.

INDEX TERMS HEMT, 2DEG charge density, band structure.

I. INTRODUCTION

Heterostructure based transistors, such as high electron mobility transistor (HEMT) and heterostructure bipolar transistor (HBT), require a careful design of the layer sequence, composition, and thickness, in order to achieve the desired band structures and the specific values of their critical parameters [1], [2]. Once the layer sequence has been grown, it has been possible to assess certain band diagram parameters such as bandgaps and band-offsets using photoemission spectroscopies, e.g., x-ray or ultra-violet photoelectron spectroscopies [3]–[6]. These spectroscopies are limited to structures of no more than two layers [7]. Spectroscopies based on absorption, overcome this limitation, but nonetheless, face another challenge. The optical transitions they detect are typically red-shifted due to the presence of high built-in electric fields, which renders the band-to-band transition spectra inaccurate for immediate band structure analysis [8]. Nonetheless, it has been shown

that surface photovoltage spectroscopy (SPS) could still be used successfully to this end when augmented with numerical simulations [9]–[11]. In most of the practical cases, however, developers of heterostructure devices rely on simulations alone, with their only feedback coming from electrical characterization of fully fabricated devices [12]–[14]. Here, we present a *fully empirical* method that *does not require simulations*. It also *does not require any fabrication* process and may be carried out on as-grown wafers.

We have recently introduced the channel photocurrent spectroscopy method that provides the desired information not only at equilibrium but also under all operating conditions of the transistor [15]. That method was based on measurement of photocurrent in the HEMT channel under various gate voltages, and therefore required a *full transistor fabrication*. Here, we present a *contactless* method, based on surface photovoltage spectroscopy that provides the desired parameters of the transistor in *equilibrium* [16].

The advantage of the proposed method is in its ability to provide feedback on the structure and its properties right after the growth. Thus, it may be used to screen out low performance wafers saving the cost and the time of a full fabrication process.

Both the theoretical and the experimental parts of this work will be presented for the special case of a plain AlGaIn/GaN HEMT structure, without limiting the generality of the method which is suitable for many other combinations and numbers of different semiconductor layers.

II. MODEL

Upon absorption of light in an AlGaIn/GaN HEMT structure, electron-hole pairs are generated in either the GaN or the AlGaIn layers. The photo-generated pairs are separated by the internal electric fields in the layers. The electrons are transferred by the internal electric fields towards the quantum well (QW), increasing the carrier concentration in the well. At the same time, holes are swept away from the heterojunction. The resulting rise in the 2-dimensional electron gas (2DEG) electron concentration increases the conductivity in the channel. Under a constant drain-to-source voltage this excess charge gives rise to a photocurrent. The same charge separation also modifies the built-in fields resulting in changes to the band bending of both layers, which is observed as a change in the surface photovoltage.

The channel photocurrent may be expressed in terms of the carrier concentration in the 2DEG¹:

$$I_{PH}(h\nu) = V_{DS} \cdot q \cdot \Delta n_S(h\nu) \cdot \mu \frac{W}{L} \quad (1)$$

where V_{DS} is the drain-source voltage, q – the electron charge, $\Delta n_S(h\nu)$ – photo-generated excess sheet charge concentration in the 2DEG, μ – electron mobility in the 2DEG, L and W are the length and width of the 2DEG channel, respectively.

We have previously modeled the effect of the built in fields on photon absorption and its manifestation in the *channel photo-current* [15]. The same effect may actually be observed using any spectroscopy that is related to absorption of photons in a semiconductor. It causes the band-to-band photo-response to commence well below the bandgap energy and increase gradually towards the actual bandgap energy. The generated excess carriers give rise to a photocurrent given by [15]:

$$I_{PH}(h\nu) = I_{PH}(E_g) \exp \left[- \left(\frac{E_g - h\nu}{\Delta E} \right)^{3/2} \right] \quad (2)$$

where I_{PH} is the measured photocurrent normalized to the surface reflectance, i.e., divided by the surface transmission

1. Eq. (1) is based on Ohm's law, $I=V/R$. Since the resistor is a quantum well, its resistivity is defined using sheet charge density rather than the common 3D charge density: $1/R = \sigma A/L = (q \cdot \mu \cdot \Delta n/t)(t \cdot W)/L$, where t – the thickness of the well – cancels out.

$1 - R(h\nu)$,² $I_{PH}(E_g)$ is the photocurrent at the bandgap photon energy following the rise, $R(h\nu)$ – spectral reflectance from the sample surface, E_g – the bandgap energy of the layer material, $h\nu$ – the photon energy, and ΔE is given by:

$$\Delta E = \left[\frac{3qF\hbar}{4\sqrt{2m}} \right]^{2/3} \quad (3)$$

where F is the built-in field, \hbar – the reduced Planck constant, and m^* is the reduced effective mass in the layer material. Combining Eqs. (1) and (2), we get an expression for the photo-generated excess carrier concentration in the 2DEG as a function of photon energy:

$$\Delta n_S(h\nu) = \Delta n_S(E_g) \exp \left[- \left(\frac{E_g - h\nu}{\Delta E} \right)^{3/2} \right] \quad (4)$$

Photo-generated excess carriers in the 2DEG affect the electric field and, consequently, the band bending in the layer. As the top AlGaIn layer holds at both ends equal charges of opposite signs (ionized surface states vs. 2DEG charge), it may be treated as a parallel-plate capacitor.³ The GaN layer, on the other hand, is in a state of accumulation at the interface with the AlGaIn forming a QW. The effect of electric field on absorption is the strongest at the point where the electric field is the highest. The maximum electric field is reached at the interface. However at that point, electrons cannot be excited to the conduction band minimum, because the first eigenstate is higher than the bottom of the conduction band. The lowest energy point for the first eigenstate is where it meets the bottom of the conduction band, which is therefore the point where absorption starts. Within an infinitesimally small depth around this point the band bending may be assumed linear. Hence, the electric field around this point will be approximately constant. In each of the layers, the electric displacement field may generally be expressed by [17]:

$$\vec{D} = \epsilon_S \vec{F} + \sum \vec{P} \quad (5)$$

where \vec{D} is the electric displacement field, $\sum \vec{P}$ – the sum of spontaneous, \vec{P}_{SP} , and piezoelectric, \vec{P}_{PE} , polarization vectors (which are present only in polar materials), and ϵ_S is the permittivity of the layer material. Rewriting Eq. (5) in terms of the 2DEG sheet charge density we get:

$$n_S + \Delta n_S(h\nu) = \frac{1}{q} \left(\epsilon_S \frac{\phi_{BBD} + \Delta \phi_{BB}(h\nu)}{t} + \sum \vec{P} \right) \quad (6)$$

where n_S – 2DEG sheet charge density in dark, ϕ_{BBD} – potential across the layer in dark, $\Delta \phi_{BB}(h\nu)$ – change in

2. Not all the impinging light crosses the surface into the semiconductor. Some of it, R , is reflected, and only $1-R$ of it, which we denote as surface transmission, actually contributes to absorption. Since the reflectance has wavelength dependence, we have to normalize by $1-R$ to remove its effect on the photocurrent.

3. Since the AlGaIn layer is unintentionally doped, the effect of ionized dopants on the electric field is negligible compared to the effect of the polarization induced charges at the two surfaces.

the layer potential upon illumination with photons of energy, $h\nu$, and t – the layer thickness. Piecewise representation of Eq. (6) yields:

$$\begin{cases} n_S = \frac{1}{q} \left(\varepsilon_S \frac{\phi_{BB}}{t} + \sum \vec{P} \right) \\ \Delta n_S(h\nu) = \frac{\varepsilon_S \Delta \phi_{BB}(h\nu)}{qt} \end{cases} \quad (7)$$

Substituting Eq. (7) into Eq. (4), we obtain an expression for the effect of the built-in field (Franz-Keldysh effect) on the photovoltage:

$$\Delta \phi_{BB}(h\nu) = \Delta \phi_{BB}(E_g) \exp \left[- \left(\frac{E_g - h\nu}{\Delta E} \right)^{3/2} \right] \quad (8)$$

where $\Delta \Phi_{bb}(E_g)$ is the change in the potential across the layer observed when the photon energy equals the bandgap energy, surface transmission normalized (divided by $1-R(h\nu)$).

Equation (8) may be transformed into the following linear form:

$$y(h\nu) = \left[\ln \left(\frac{\Delta \phi_{BB}(E_g)}{\Delta \phi_{BB}(h\nu)} \right) \right]^{2/3} = \frac{E_g - h\nu}{\Delta E} \quad (9)$$

The slope of the linear function in Eq. (9) may then be used in Eq. (3) to obtain the electric field in the layer. Once the electric fields in both the GaN and the AlGa_N layers are known, the 2DEG charge density is readily obtained from the discontinuity in the electric displacement field across the interface [18], [19]:

$$\begin{aligned} qn_S = & \left(\varepsilon_S \vec{F}_{AlGaN} + \vec{P}_{SP,AlGaN} + \vec{P}_{PE,AlGaN} \right) \\ & - \left(\varepsilon_S \vec{F}_{GaN} + \vec{P}_{SP,GaN} \right) \end{aligned} \quad (10)$$

where \vec{F}_{AlGaN} , $\vec{P}_{SP,AlGaN}$, and $\vec{P}_{PE,AlGaN}$ are electric field, spontaneous, and piezoelectric polarization in the AlGa_N, and \vec{F}_{GaN} , and $\vec{P}_{SP,GaN}$ are the electric field, and the spontaneous polarization in GaN, respectively.

III. EXPERIMENT

To test the model experimentally, we used a AlGa_N/GaN heterojunction. The heterostructure was grown by metal organic chemical vapor deposition (MOCVD) on c-plane sapphire. The layer sequence was an AlN nucleation layer, 2 μm of undoped GaN, 11 nm of Al_{0.3}Ga_{0.7}N, and 1.5 nm GaN cap layer. Device fabrication and details of the spectroscopic setup have been described elsewhere [15]. Photocurrent was measured on 17 transistors on the same wafer. Surface photovoltage was measured on as grown wafers using a Kelvin probe (Besoke Delta Phi GmbH) in the same spectrometric system under identical illumination conditions as the photocurrent. Further details of the surface photovoltage method and its physics may be found in [16]. Photovoltage measurements were carried out on 7 different locations on the same wafer.

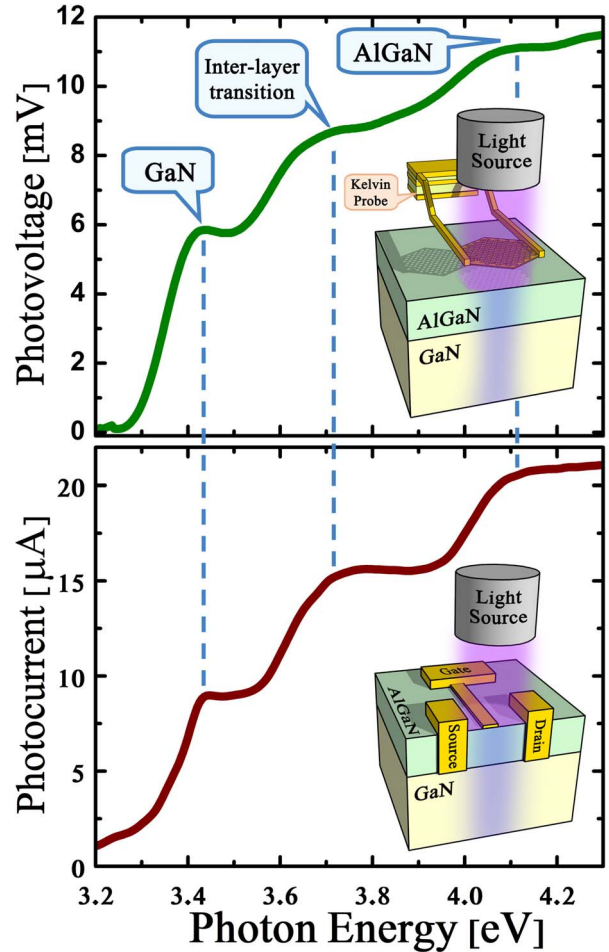


FIGURE 1. Top – surface photovoltage spectrum acquired from an as grown AlGa_N/GaN structure grown on sapphire. It shows a set of 3 steps. Each step ends at a transition energy. The first and the last transition energies are the GaN and the AlGa_N bandgap, respectively. Between them there supposed to be two inter-layer transitions. However, one of these transitions is weak and only the other can be clearly distinguished (from AlGa_N valence band to GaN conduction band). The inset shows the layer structure with a cartoon of the semitransparent Kelvin probe and a spectrometric light source. Bottom – photocurrent measured in the channel of a HEMT transistor fabricated on the same wafer and measured in the same spectroscopic system and under the same conditions as the photovoltage. The photocurrent shows the same steps at the same energies. The inset shows the transistor illuminated from the gate side.

IV. RESULTS AND DISCUSSION

A photovoltage spectrum, measured on an unpatterned area of the wafer, and normalized to the surface transmission, is shown on Fig. 1a. Figure 1b shows a surface-transmission normalized photocurrent spectrum obtained from a transistor fabricated on the same wafer. Similar step responses of GaN, AlGa_N and AlGa_N/GaN inter-layer transitions are observed in both spectra. In both spectra the steps are not sharp, but rather preceded by a gradual increase. We have shown before that the slope preceding each photocurrent step is a result of electric-field-assisted absorption, also known as the Franz-Keldysh effect, and may be used to measure the electric field in the corresponding layer [20]. Here, we compare results from the previously established photocurrent

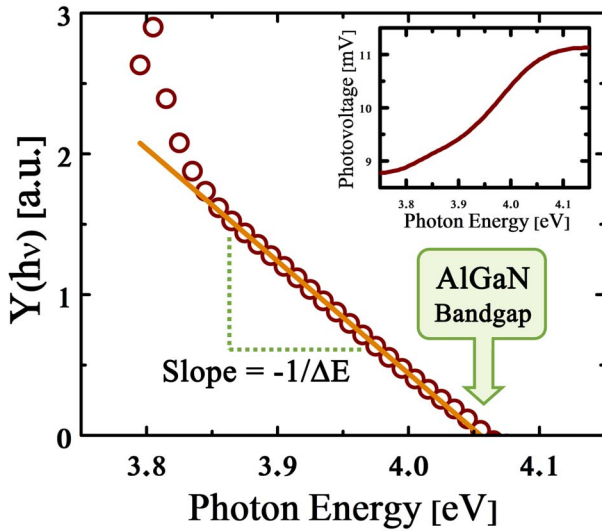


FIGURE 2. A linear representation of the photovoltage step response of AlGaIn layer (The original photovoltage response is shown in the inset) using Eq. (9). The intersect of the linear curve with the photon energy axis is at the bandgap of the material. The slope of the linear curve may be used to calculate the built-in field in the layer.

method to those obtained from surface photovoltage. To obtain the built-in fields from the photovoltage spectrum, we used Eq. (9) which transforms the slope preceding the bandgap energy into a linear curve. Figure 2 shows the linear form of the photovoltage step response of AlGaIn layer (circles). The linearity of the curve provides graphical confirmation to the assumption that the physics underlying the shape of the step is indeed the Franz-Keldysh effect. A solid line shows the linear fit. According to Eq. (9), the linear curve intersects the photon energy axis at the bandgap, while the slope may be used with Eq. (3) to calculate the built-in electric field in the layer. Using this graphical method yields an electric field of $0.596 \pm 0.018 \text{ MV/cm}$ in the GaN layer and $1.318 \pm 0.031 \text{ MV/cm}$ in the AlGaIn layer. For comparison, the electric fields obtained from photocurrent spectrum using the photocurrent model [15] were 0.597 ± 0.036 and $1.374 \pm 0.018 \text{ MV/cm}$ for GaN and AlGaIn layers, respectively.

Bandgaps obtained from the intersection of linear fit with the photon energy axis for the spectral data shown in Fig. 1 were 4.05 eV for AlGaIn and 3.43 eV for GaN. The AlGaIn/GaN interlayer transition at 3.68 eV suggests a valence band offset of $\Delta E_V = 0.15 \text{ eV}$. The other interlayer transition is rather weak in both spectra. The 2DEG sheet charge densities calculated using Eq. (10) from the photovoltage and photocurrent data are $9.78(\pm 0.27) \cdot 10^{12} \text{ cm}^{-2}$ and $9.47(\pm 0.32) \cdot 10^{12} \text{ cm}^{-2}$, respectively. The values of the polarization vectors used in the calculation were -0.0340 C/m^2 , -0.0464 C/m^2 and -0.0098 C/m^2 for $P_{SP, \text{GaN}}$, $P_{SP, \text{AlGaIn}}$ and $P_{PE, \text{AlGaIn}}$ (Al composition of 30%), respectively [21]. The values obtained with the two methods are within measurement error from one another.

Using the photovoltage method on AlGaIn/GaN structure, we obtained the bandgaps, band offsets and built-in electric

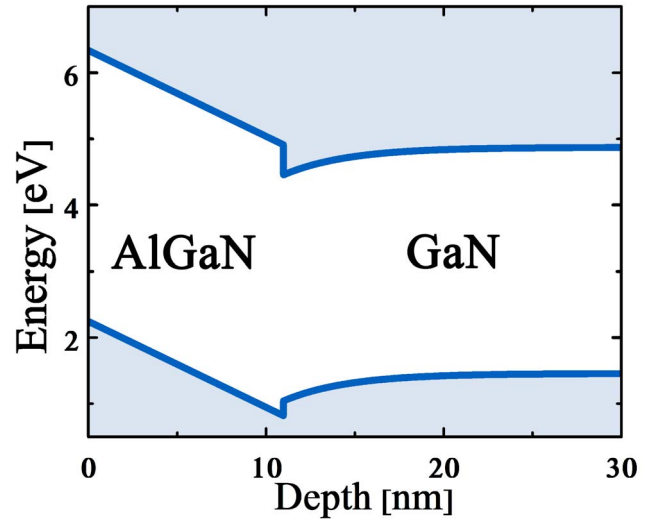


FIGURE 3. An equilibrium band diagram of the AlGaIn/GaN HEMT structure calculated from the photovoltage data.

fields in the structure and verified their accuracy comparing them to the same parameters obtained using the photocurrent method. Figure 3 shows the resulting equilibrium band diagram of the HEMT structure that corresponds to these values. The potential in the AlGaIn was assumed linear, while for the GaN potential we used a one-dimensional Schrodinger-Poisson solver. The input parameter used in the solver, was the electric field measured in the GaN at the intersection of the first sub-band energy in the GaN quantum well with the conduction band.

V. CONCLUSION

Within our measurement error, both the photocurrent and the photovoltage methods provided the same values of the internal electric fields and the 2DEG sheet charge density. Although, at first sight, both methods appear to yield very similar spectra, the photovoltage method holds a major advantage over the photocurrent method by being contactless. It does not require the fabrication of a transistor or even of Ohmic contacts. Using photovoltage, the most significant transistor parameters can be measured at the bare wafer stage, before any fabrication step has taken place. Nonetheless, this method is limited to equilibrium conditions. To evaluate the dependence of these parameters on the gate voltage, one would still need the photocurrent method that requires the full fabrication of a transistor. Hence, the photovoltage method may serve for pre-fabrication screening of wafers, whereas the photocurrent method may be used for full-blown post-fabrication studies. Photovoltage scan of the wafer may provide a map of the wafer to evaluate the lateral uniformity of the 2DEG charge density. Finally, the method presented here is by no means limited to characterization of HEMT structures, but should be suitable to any modern multi-layer device, e.g., heterojunction bipolar transistor, multi-quantum well LED, etc.

REFERENCES

- [1] J. A. del Alamo, "Nanometre-scale electronics with III–V compound semiconductors," *Nature* vol. 479, pp. 317–323, Nov. 2011, doi: [10.1038/nature10677](https://doi.org/10.1038/nature10677).
- [2] U. K. Mishra, L. Shen, T. E. Kazior, and Y.-F. Wu, "GaN-based RF power devices and amplifiers," *Proc. IEEE*, vol. 96, no. 2, pp. 287–305, Feb. 2008, doi: [10.1109/JPROC.2007.911060](https://doi.org/10.1109/JPROC.2007.911060).
- [3] L. Sun *et al.*, "Band alignment of SnS/Zn(O,S) heterojunctions in SnS thin film solar cells," *Appl. Phys. Lett.*, vol. 103, no. 18, 2013, Art. no. 181904, doi: [10.1063/1.4821433](https://doi.org/10.1063/1.4821433).
- [4] T. D. Veal *et al.*, "Valence band offset of the ZnO/AlN heterojunction determined by x-ray photoemission spectroscopy," *Appl. Phys. Lett.*, vol. 93, no. 20, 2008, Art. no. 202108, doi: [10.1063/1.3032911](https://doi.org/10.1063/1.3032911).
- [5] Y.-Y. Zhang, L.-X. Qian, and X.-Z. Liu, "Determination of the band alignment of a-IGZO/a-IGMO heterojunction for high-electron mobility transistor application," *Physica Status Solidi RRL*, vol. 11, no. 10, 2017, Art. no. 1700251, doi: [10.1002/pssr.201700251](https://doi.org/10.1002/pssr.201700251).
- [6] K. Sawangri *et al.*, "Experimental band alignment of Ta2O5/GaN for MIS-HEMT applications," *Microelect. Eng.*, vol. 178, pp. 178–181, Jun. 2017, doi: [10.1016/j.mee.2017.04.010](https://doi.org/10.1016/j.mee.2017.04.010).
- [7] W. Mönch, *Electronic Properties of Semiconductor Interfaces*. Berlin, Germany: Springer, 2004, pp. 79–80.
- [8] D. Cavalcoli, S. Pandey, B. Fraboni, and A. Cavallini, "Band gap shift in Al_{1-x}In_xN/AlN/GaN heterostructures studied by surface photovoltage spectroscopy," *Appl. Phys. Lett.*, vol. 98, no. 14, 2011, Art. no. 142111, doi: [10.1063/1.3576938](https://doi.org/10.1063/1.3576938).
- [9] S. Solodky *et al.*, "Characterization methodology for pseudomorphic high electron mobility transistors using surface photovoltage spectroscopy," *J. Appl. Phys.*, vol. 88, no. 11, pp. 6775–6780, 2000, doi: [10.1063/1.1324696](https://doi.org/10.1063/1.1324696).
- [10] S. Solodky *et al.*, "Surface photovoltage spectroscopy of epitaxial structures for high electron mobility transistors," *Appl. Phys. Lett.*, vol. 83, no. 12, pp. 2465–2467, 2003, doi: [10.1063/1.1613794](https://doi.org/10.1063/1.1613794).
- [11] S. Solodky *et al.*, "Surface photovoltage spectroscopy of metamorphic high electron mobility transistor structures," *J. Vac. Sci. Technol. B*, vol. 22, no. 5, p. 2434, 2004, doi: [10.1116/1.1787518](https://doi.org/10.1116/1.1787518).
- [12] M. Grupen, "GaN high electron mobility transistor simulations with full wave and hot electron effects," *IEEE Trans. Electron Devices*, vol. 63, no. 8, pp. 3096–3102, Aug. 2016, doi: [10.1109/TED.2016.2581591](https://doi.org/10.1109/TED.2016.2581591).
- [13] N. M. Shrestha, Y. Li, and E. Y. Chang, "Simulation study on electrical characteristic of AlGaN/GaN high electron mobility transistors with AlN spacer layer," *Jpn. J. Appl. Phys.*, vol. 53, no. 4, 2014, Art. no. 04EF08, doi: [10.7567/JJAP.53.04EF08](https://doi.org/10.7567/JJAP.53.04EF08).
- [14] S. Yamakawa, S. Goodnick, S. Aboud, and M. Saraniti, "Quantum corrected full-band cellular Monte Carlo simulation of AlGaN/GaN HEMTs," *J. Comput. Electron.*, vol. 3, nos. 3–4, pp. 299–303, 2004, doi: [10.1007/s10825-004-7065-6](https://doi.org/10.1007/s10825-004-7065-6).
- [15] Y. Turkulets and I. Shalish, "Probing dynamic behavior of electric fields and band diagrams in complex semiconductor heterostructures," *J. Appl. Phys.*, vol. 123, no. 2, 2018, Art. no. 024301, doi: [10.1063/1.5013274](https://doi.org/10.1063/1.5013274).
- [16] L. Kronik and Y. Shapira, "Surface photovoltage phenomena: Theory, experiment, and applications," *Surface Sci. Rep.*, vol. 37, nos. 1–5, pp. 1–206, 1999, doi: [10.1016/S0167-5729\(99\)00002-3](https://doi.org/10.1016/S0167-5729(99)00002-3).
- [17] F. Bernardini, "Spontaneous and piezoelectric polarization: Basic theory vs. practical recipes," in *Nitride Semiconductor Devices*, J. Piprek, Ed. Weinheim, Germany: Wiley, 2007, p. 55.
- [18] O. Ambacher and V. Cimalla, "Polarization induced effects in GaN-based heterostructures and novel sensors," in *Polarization Effects in Semiconductor Devices*, C. Wood and D. Jena, Eds. New York, NY, USA: Springer, 2007, pp. 27–110.
- [19] U. Mishra and J. Singh, *Semiconductor Device Physics and Design*. Dordrecht, The Netherlands: Springer, 2008, pp. 375–394.
- [20] Y. Turkulets, T. Bick, and I. Shalish, "Double surface effect causes a peak in band-edge photocurrent spectra: A quantitative model," *J. Phys. D Appl. Phys.*, vol. 49, no. 36, 2016, Art. no. 365104, doi: [10.1088/0022-3727/49/36/365104](https://doi.org/10.1088/0022-3727/49/36/365104).
- [21] O. Ambacher *et al.*, "Pyroelectric properties of Al(In)GaN/GaN hetero- and quantum well structures," *J. Phys. Condens. Matter*, vol. 14, no. 13, p. 3399, 2002, doi: [10.1088/0953-8984/14/13/302](https://doi.org/10.1088/0953-8984/14/13/302).



YURY TURKULETS is currently pursuing the Ph.D. degree in electrical engineering with the Ben-Gurion University of the Negev, Israel.



ILAN SHALISH received the Ph.D. degree in electrical engineering from Tel Aviv University. He is currently an Assistant Professor with the Department of Electrical and Computer Engineering, Ben-Gurion University of the Negev, Beer Sheva, Israel. He is the member of the American Physical Society and the Material Research Society.